Hydrometallurgy 215 (2023) 105989

Contents lists available at ScienceDirect

Hydrometallurgy

journal homepage: www.elsevier.com/locate/hydromet

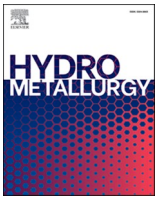

Water leaching of roasted vanadium slag: Desiliconization and precipitation of ammonium vanadate from vanadium solution

Longjie Liu [a], Toni Kauppinen [a,b], Pekka Tynjälä [a,b], Tao Hu [a], Ulla Lassi [a,b,*]

[a] University of Oulu, Research unit of Sustainable Chemistry, PO Box 4300, FI-90570 Oulu, Finland
[b] University of Jyvaskyla, Kokkola University Consortium Chydenius, Talonpojankatu 2B, FI-67100 Kokkola, Finland

ARTICLE INFO

Keywords:
Vanadium slag
Water leaching
Desiliconization
Precipitation
Vanadate

ABSTRACT

This research investigated water leaching of roasted vanadium slag and studied the effects of leaching parameters, such as agitation speed, temperature, liquid-to-solid ratio, and leaching time. Further, solution purification via desiliconization and precipitation of ammonium vanadate were studied using the vanadium solution obtained from the water leaching of roasted vanadium slag. Vanadium solution contains residual silicon (1.67 g/L), which should be removed before ammonium vanadate precipitation. Based on the results, vanadium can be effectively recovered from vanadium slag and a recovery efficiency of 96.9% was obtained under optimal water leaching conditions. During solution purification, silicon can be precipitated with $Al_2(SO_4)_3$ to very low levels without any significant vanadium loss. The ammonium vanadate precipitation achieved a high precipitation efficiency of >99%.

1. Introduction

Vanadium is widely used in many industrial applications because of its physical properties, e.g., high tensile strength, hardness, and fatigue resistance (Li et al., 2016; Liu et al., 2017; Liu et al., 2013). The demand for vanadium products is growing rapidly, especially in the high-technology fields. In addition, there is significant potential for vanadium applications as an energy storage material, with the vanadium flow battery currently considered to be one of the most promising energy storage technologies. Battery grade vanadate requires high levels of purity (Lübke et al., 2016; Wei et al., 2014; Yan et al., 2017). Worldwide demand for vanadium is expected to double over the next 10 years. Currently, the main raw material for vanadium extraction is titanomagnetite, which accounts for about 88% of vanadium production (Liu et al., 2013). During steelmaking, vanadium compounds are oxidized and enriched with oxygen lances into steel slag in a heat-resistant shaking ladle. This vanadium-bearing steel slag (called vanadium slag) is a by-product of steelmaking, and it is a direct source for vanadium extraction (Li et al., 2016).

The current process of industrial vanadium extraction from vanadium slag involves Na_2CO_3-Na_2SO_4-NaCl added oxidation roasting in air at about 800 °C, followed by water leaching and purification (Ji et al., 2017; Yang et al., 2014). The melting points of Na_2CO_3, Na_2SO_4, and NaCl are 851 °C, 884 °C, and 801 °C, respectively. It has been reported that the insoluble V^{3+} in vanadium slag is converted into soluble V^{5+} during oxidation roasting, and the vanadium extraction percentage for the traditional process is about 80% (Liu et al., 2017; Ji et al., 2017). The Na_2SO_4 and NaCl additives may produce corrosive gases, such as HCl, Cl_2, SO_2, and SO_3, which may pollute the environment. Furthermore, the traditional vanadium slag has very high chromium content, with about 5% of that chromium extracted during oxidation roasting, and the Cr^{6+} formed in the process is a major threat to human and animal health as it becomes a carcinogen upon inhalation or ingestion (Chen et al., 2013).

This study used vanadium slag with a high vanadium content from iron processing. The roasted vanadium slag was water leached. Desiliconization and precipitation of ammonium vanadate were also studied using the vanadium solution obtained from the water leaching of the vanadium slag. The research objective is to study the key parameters that affect desiliconization to decrease the Si content and the subsequent process of ammonium vanadate precipitation.

2. Materials and methods

2.1. Roasted vanadium slag

The vanadium slag (a by-product of the iron refining process) used in

* Corresponding author at: University of Oulu, Research unit of Sustainable Chemistry, PO Box 4300, FI-90570 Oulu, Finland.
E-mail addresses: toni.kauppinen@oulu.fi (T. Kauppinen), pekka.tynjala@oulu.fi (P. Tynjälä), tao.hu@oulu.fi (T. Hu), ulla.lassi@oulu.fi (U. Lassi).

https://doi.org/10.1016/j.hydromet.2022.105989
Received 11 September 2020; Received in revised form 24 October 2022; Accepted 25 October 2022
Available online 29 October 2022

this study was provided by a Finnish company. It was first ground and screened using Tyler standard screens (60 mesh, 120 mesh, and 200 mesh, i.e. 250 μm, 125 μm, and 74 μm). The vanadium slag was soda roasted (Fig. 1) at 1300 °C for one hour before water leaching, followed by purification of the vanadium solution via desiliconization. Ammonium vanadate was then precipitated from the vanadium solution.

2.2. Water leaching experiments

The process parameters for the water leaching of roasted vanadium slag (temperature, L/S ratio, agitation speed) were optimized for best vanadium yield. Table 1 shows the leaching conditions and variables studied.

All water leaching experiments were performed in a 0.5 L cylindrical stainless steel autoclave equipped with a temperature control unit, an electric heating furnace, a magnetic driven agitator, and a cooling tube system. The temperature control unit comprises a thermocouple and a regulator for the heating furnace. The reaction temperature was kept constant with a precision of ±1 °C.

The leaching experiments were conducted using 20–50 g of roasted vanadium slag particles and 200 g of ultrapure water. The ultrapure water was heated up to a preset temperature, the vanadium slag was then added, and the timing of the leaching commenced. After leaching, the slurry was filtered and washed, and the resulting liquid (vanadium solution) was analyzed. Furthermore, the residue left behind after water leaching was characterized using X-ray fluorescence (XRF).

The vanadium yield from the vanadium slag was calculated using the following eq.

$$X = \left(1 - [C]_r/[C]_0\right) \times 100\% \quad (1)$$

where $[C]_r$ and $[C]_0$ are the vanadium content (mg/g) in the residue and in the original vanadium slag, respectively.

The effects of agitation speed, temperature, and liquid-to-solid ratio on the vanadium yield were investigated via experiments at agitation speeds of 300 rpm, 500 rpm, and 700 rpm, and liquid-to-solid ratios of 3:1, 4:1, 5:1, and 10:1. Leaching experiments were performed within a temperature range of 60 °C to 100 °C.

2.3. Solution purification via desiliconization

The vanadium solution obtained after the water leaching still contains a large amount of silicon, which should be removed before vanadate precipitation. Desiliconization was performed using aluminum sulfate hydrate ($Al_2(SO_4)_3$, Sigma Aldrich, 98%). The effects of temperature, pH, $Al_2(SO_4)_3$/Si mass ratio, agitation speed, and desiliconization time were studied (see Table 2).

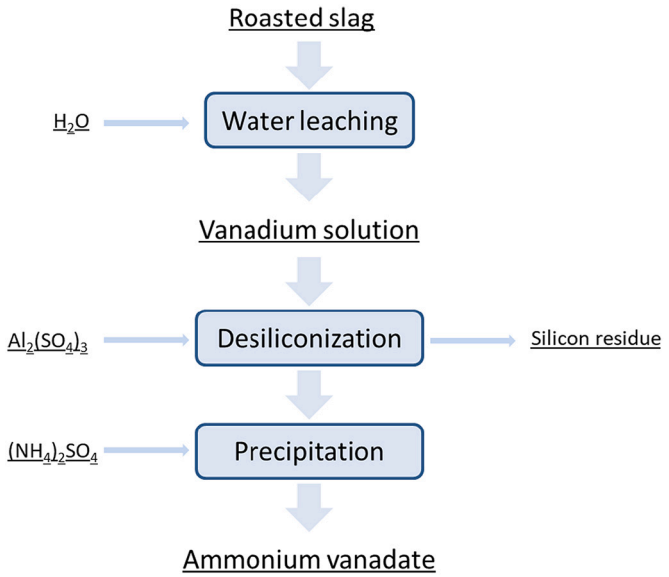

Fig. 1. Scheme for vanadium slag processing.

Table 1
Selected optimal leaching conditions and studied variables.

Leaching temperature (°C)	Liquid-to-solid ratio	Time (min)	Agitation speed (rpm)	Presentation of results
80	10:1	60	variable	Fig. 3a
variable	10:1	60	500	Fig. 3b
100	variable	60	500	Fig. 3c
100	4:1	variable	500	Fig. 3d

Particle size below 200 mesh (74 μm) for leaching

2.4. Precipitation experiments

In producing V_2O_5, the process of precipitating vanadium from sodium vanadate solution is very crucial. Vanadium precipitation methods include hydrolysis precipitation and ammonium salt precipitation. There are three different ammonium salt precipitation techniques, including ammonium vanadate in alkaline solution technique, weak acid precipitation, and acid precipitation.

In this study, the ammonium salt (NH_4Cl) assisted precipitation method was used to obtain high quality V_2O_5. Using acid or ammonium salt to adjust the pH of sodium vanadate to a different pH values (7.0–9.0) yield different types of ammonium polyvanadate.

2.5. Characterization methods

The composition of the vanadium slag and solid residues were analyzed via digestion and inductively coupled plasma optical emission spectrometry (ICP-OES), using a Perkin Elmer Optima 5300 DV ICP–OES instrument, and via XRF, using a Bruker AXS S4 Pioneer X-Ray Fluorescence Spectrometer. The mineralogical phases of vanadium slag and the solid residues were examined via X-ray diffraction (XRD) (PANalytical X'Pert Pro X-ray diffractometer, Malvern Panalytical) using monochromatic CuKα1 radiation (λ = 1.5406 Å) at 45 kV and 40 mA. Diffractograms were captured in the 2θ range, 10–90°, at 0.017° intervals, with scan step time of 100 s. The crystalline phases and structures were analyzed using HighScore Plus software (Version 4.0, PANalytical B.V., Almelo, The Netherlands) and with standard files complied by the International Centre for Diffraction Data (ICDD).

3. Results and discussion

3.1. Water leaching

The aim of the roasting was to convert the vanadium into soluble form. The composition of the vanadium slag before and after the soda roasting are presented in Table 3. The XRD of the vanadium slag before soda roasting is presented in Fig. 2a. Vanadium slag contains a substantial amount of vanadium, iron, manganese, aluminum, and silicon. The research results show that the main phases in the converted vanadium slag were the spinel phase, silicate phase, and inclusion phase. The vanadium was predominantly V_3O_4, a spinel phase similar to FeV_2O_4 (Macdougall et al., 2012).

The XRD of the soda-roasted vanadium slag, which indicates the presence of water-soluble Na_3VO_4, is presented in Fig. 2b. After roasting, the vanadium content in the slag decreased and the sodium content increased significantly.

Based on the XRD data, the vanadium in the vanadium slag was in the form of Fe—V spinels wrapped in silicates (olivine phase) and a minor phase (V_2O_3 and VO). During alkali roasting, silicates in the outer layer decomposed, and an acmite ($NaFeSi_2O_6$) phase formed when the

Table 2
Selected optimal conditions for desiliconization and studied variables.

Desiliconization temperature (°C)	pH	$Al_2(SO_4)_3$/Si mass ratio	Agitation speed (rpm)	Desiliconization time (min)	Presentation of results
80	variable	10	500	240	Fig. 5a
80	8.0	variable	500	240	Fig. 5b
variable	8.0	15	500	240	Fig. 5c

Table 3
Chemical composition of vanadium slag before and after soda roasting.

Component	Na_2O	MgO	Al_2O_3	SiO_2	P_2O_5	CaO	TiO_2	V_2O_5	Cr_2O_3	MnO	FeO
Before roasting wt (%)	0.08	4.04	1.59	14.3	0.24	2.71	0.68	30.9	1.1	5.36	29.9
After roasting wt (%)	33.9	1.03	0.24	10.9	0.09	1.37	2.94	19.9	0.71	3.23	35.1

(200 mesh, 74 μm).

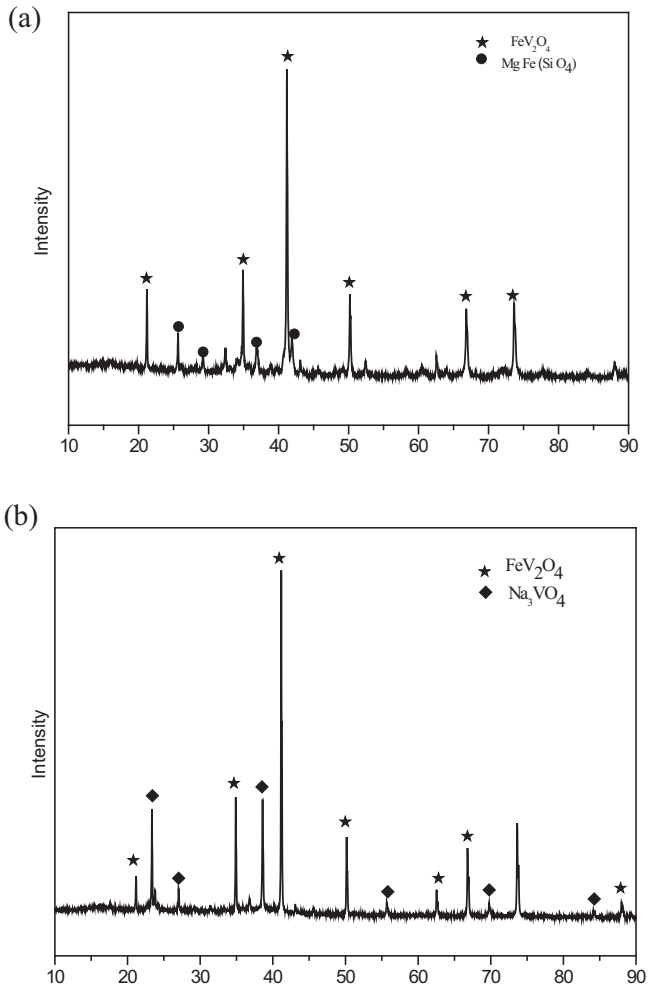

Fig. 2. XRD scans of the vanadium slag a) before and b) after roasting (200 mesh, 74 μm).

temperature was 700 °C. As the roasting temperature rose to 900 °C, the major phases (such as Fe_2O_3 and $Ca_3TiFeSi_3O_{12}$) are observed because the higher content of Si, Ti, and Ca adversely affected the diffusion of vanadium, oxygen, and sodium.

It has been reported that the silicon and calcium content of vanadium slag can decrease the extraction percentage of vanadium due to the formation of water-insoluble sodium-iron-silicates ($Na_2O{\bullet}Fe_2O_3{\bullet}4SiO_2$) and calcium vanadate during oxidation roasting. Vanadium related reactions during alkali roasting are expressed as follows.

$$4V_3O_4 + 7O_2\ (g) = 6V_2O_5 \quad (2)$$

$$Na_2CO_3 = Na_2O + CO_2\ (g) \quad (3)$$

$$V_2O_5 + Na_2O = 2NaVO_3 \quad (4)$$

$$NaVO_3 + Na_2O = Na_3VO_4 \quad (5)$$

Water leaching was performed as described in Section 2.2. During water leaching, the dissolution of sodium vanadate in the roasted slag can slow down the leaching kinetics for vanadate. The effect of agitation speed on the leaching efficiency was studied (see Table 1). In Fig. 3a, it can be seen that the agitation speed has only a slight effect on the leaching efficiency of vanadium from the vanadium slag. When the agitation speed is 500 rpm or higher, the vanadium extraction percentage is >95%, and the vanadium content of the leach residue is 0.61% or less. The effects of temperature and liquid-to-solid ratio were studied at a constant agitation speed of 500 rpm.

The effect of temperature on the leaching efficiency was also studied (see Table 1). As shown in Fig. 3b, at a temperature of 60 °C, the vanadium content in the solid residue was higher than 1.5 wt%, and the vanadium extraction percentage increased with rising temperature. At a reaction temperature of 100 °C, the vanadium content in the residue was 0.61%, and the vanadium extraction percentage was >95%.

The effect of the liquid-to-solid ratio on the leaching efficiency was also studied (see Table 1). As shown in Fig. 3c, the effect of the L/S mass ratio on the vanadium yield was not high, as increasing the L/S ratio decreased the vanadium yield only slightly. Similarly, the vanadium content in the solid residue was <1 wt%. Finally, the effect of leaching time was studied. The vanadium leaching rate was very fast during the first 10 min of reaction, with no significant leaching after 60 min (Fig. 3d).

The XRD scans of the roasted vanadium slag after water leaching are presented in Fig. 4. Sodium vanadate (Na_3VO_4 major phase) was observed in the roasted slag (Fig. 2b) before water leaching, but $NaVO_3$ was not observed due to its low content and poor crystallinity. After water leaching, sodium vanadate was not observed in the solid residue, indicating that the vanadium had been translocated to the solution.

In conclusion, water leaching of vanadium from roasted vanadium slag was performed successfully, with a high vanadium yield (>95%). The vanadium content of the sludge residue was low (<1 wt%). Increasing the temperature increased the vanadium yield; and therefore, an optimal temperature of 100 °C was selected to avoid using pressurized conditions. As demonstrated in an earlier study by Liu et al. (Liu et al., 2017), much higher yields can be achieved under pressurized conditions. The effects of agitation speed and the liquid-to-solid ratio were only barely noticeable under the studied conditions.

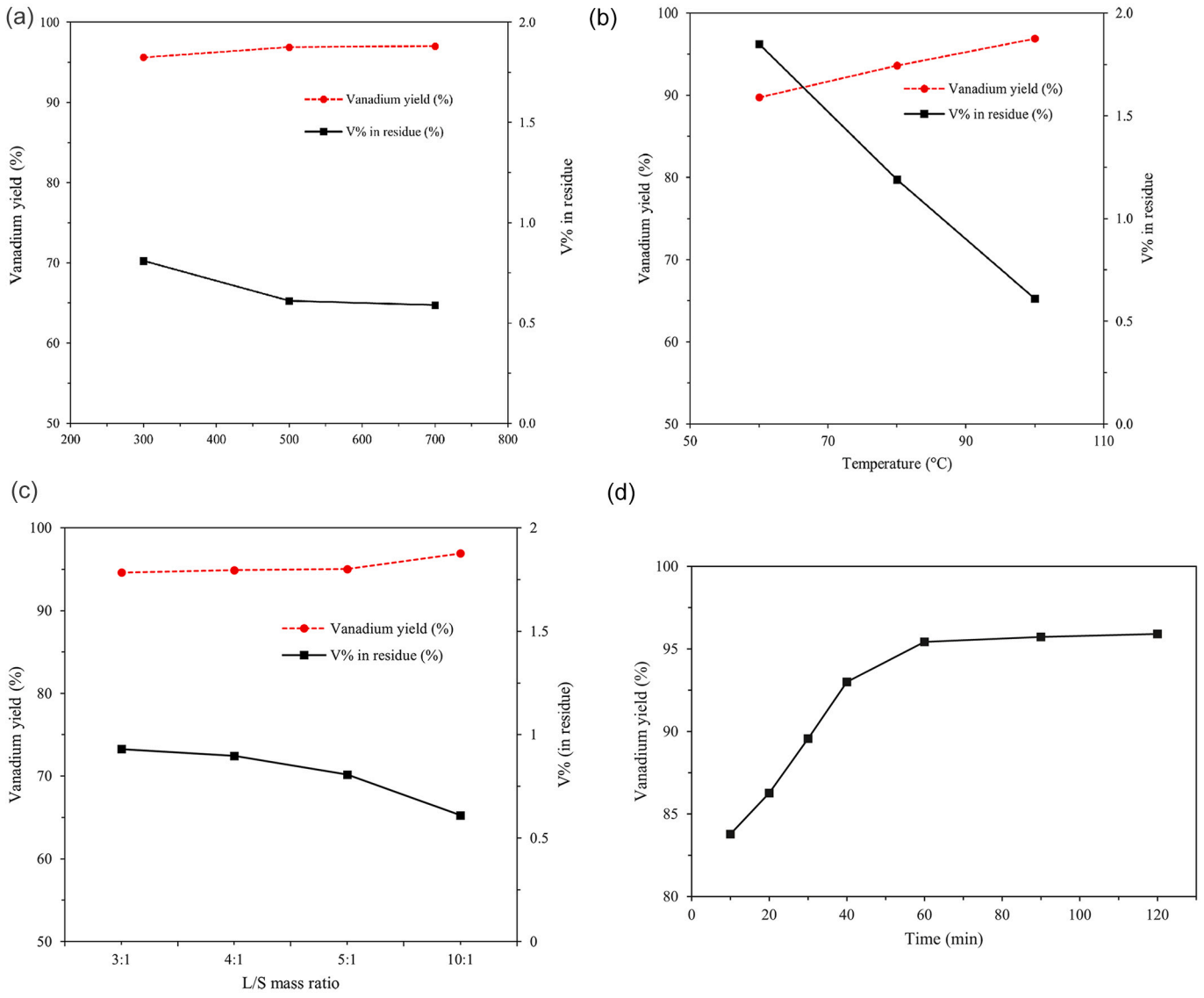

Fig. 3. Effect of a) agitation speed, b) water leaching temperature, c) L/S ratio and d) leaching time on vanadium yield and vanadium content in the solid residue.

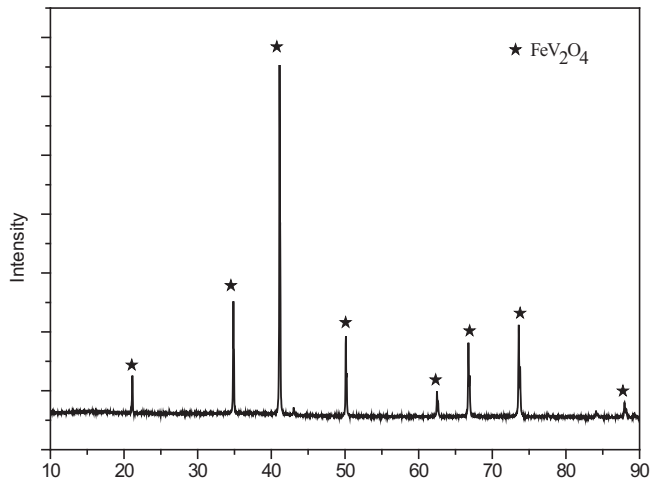

Fig. 4. XRD scan of residue after water leaching of roasted vanadium slag.

3.2. Desiliconization

Vanadium solution was obtained by repeating the steps outlined earlier under optimal reaction conditions. The vanadium solution obtained from the water leaching had the following composition: V_2O_5 content of 52.5 g/L, and silicon concentration of 1.67 g/L. Solution purification via desiliconization was performed on the vanadium solution, and the effects of pH, $Al_2(SO_4)_3$/Si mass ratio, and temperature on desiliconization were studied.

The effect of pH on the desiliconization efficiency was studied under optimal reaction conditions (see Table 2). The vanadium yield and desiliconization efficiency are plotted in Fig. 5a. As can be seen in Fig. 5a, pH affects the desiliconization efficiency considerably. Due to the agglomeration of silicon, the desiliconization efficiency decreased with increasing pH. The vanadium leaching efficiency decreased from 87.6% to 66.3% with the decrease of pH from 12 to 8. Furthermore, when the pH is high, silicon agglomerates rapidly, making filtration very difficult due to the formation of colloids. Therefore, the recommended pH for desiliconization is determined to be 9.0 to 10.5, and the silicon concentration can be as low as 0.42 g/L, with a vanadium yield of 86.3%.

The effect of the amount of added $Al_2(SO_4)_3$ on the desiliconization

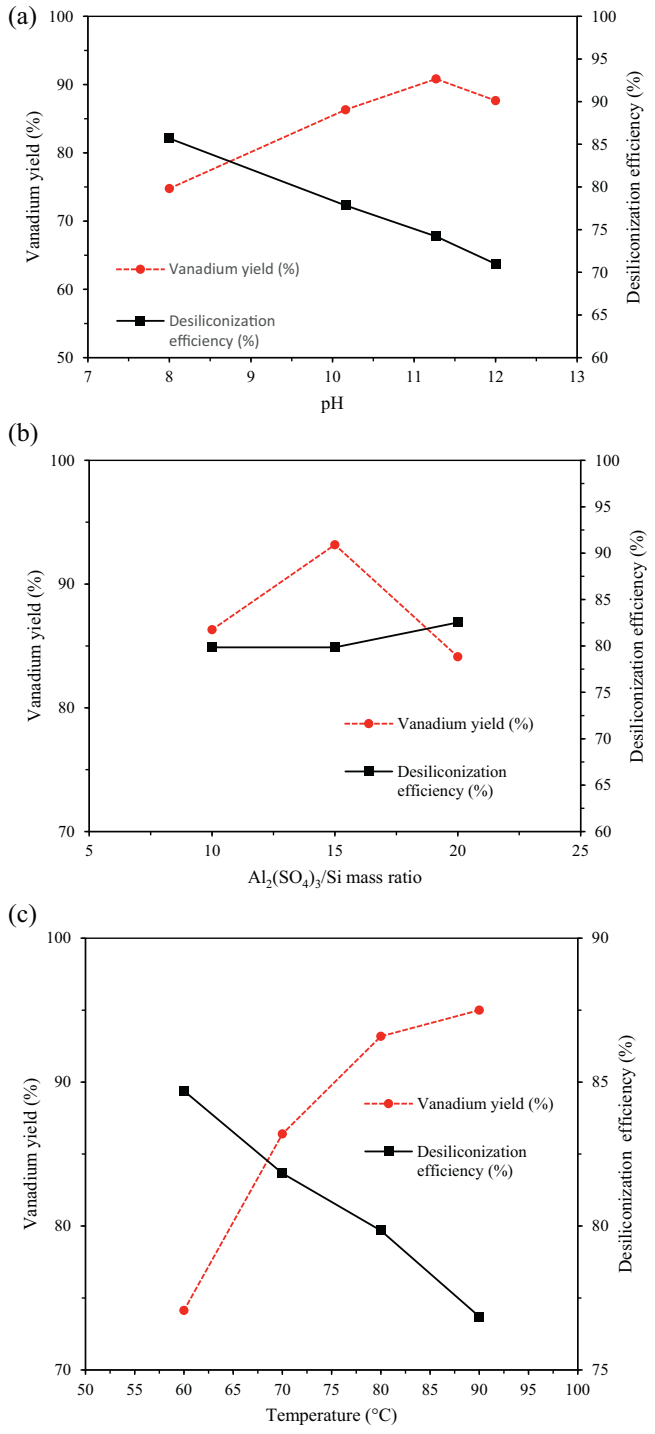

Fig. 5. Effect of a) pH, b) $Al_2(SO_4)_3$/Si mass ratio, and c) temperature on the vanadium yield (%) and desiliconization efficiency (%). Initial V_2O_5 concentration: 52.5 g/L, silicon concentration: 1.67 g/L.

efficiency and vanadium yield are plotted in Fig. 5b. The corresponding reaction conditions are shown in Table 2. As can be seen in Fig. 5b, when the $Al_2(SO_4)_3$/Si mass ratio was 10, the desiliconization efficiency was 79.9%. When the mass ratio was increased to 15, the desiliconization rate increased slightly, while the vanadium yield increased from 86.3% to 93.2%. However, further increase in the $Al_2(SO_4)_3$/Si mass ratio may decrease vanadium yield. Consequently, the optimal $Al_2(SO_4)_3$/Si mass ratio is determined to be 15.

The effect of temperature on silicon removal efficiency are shown in Fig. 5c. Corresponding reaction conditions are given in Table 2. It can be concluded from the results presented in Fig. 5c that the desiliconization is higher at lower temperatures. Significant removal of silicon was achieved at all temperatures studied. However, when the desiliconization temperature is too low (60 °C or lower), the filtration rate is very low due to the amorphous form of the precipitate. Vanadium is also lost at lower temperatures due to absorption of the precipitate. Temperatures of 70 to 80 °C are optimal for desiliconization.

In conclusion, silicon can be significantly removed from the solution during the desiliconization. The effect of all the parameters studied, such as pH, temperature, and $Al_2(SO_4)_3$/Si ratio affect the desiliconization process, showing that it is possible to get optimized conditions for silicon removal without a loss of vanadium. The composition of the remnant solution after desiliconization is presented in Table 4. As can be seen in Table 4, the content of the vanadium in the remnant solution is still high, and the residue should be carefully washed to remove all water-soluble vanadium to prevent the vanadium loss.

3.3. Precipitation of ammonium vanadate

3.3.1. Effect of pH

To obtain a high quality of V_2O_5, the ammonium salt precipitation method is used. Adjusting the pH of sodium vanadate to different levels using acid and adding ammonium salt can yield different types of ammonium polyvanadate. Table 5 lists different vanadium ion species at different pH values at a total vanadium concentration of 0.5 g/L.

The proton in polyvanadate acid can be replaced by another positive ion. For $H_2V_{12}O_{31}$, the equation is as follows.

$$H_2V_{12}O_{31} + 2\,M^+ = M_2V_{12}O_{31} + 2H^+ \quad (6)$$

The selection of the M^+ ion is as follows.

$$K^+ > NH_4^+ > Na^+ > H^+ > Li^+ \quad (7)$$

The Na^+ in $Na_2V_{12}O_{31}$ can be replaced with NH_4^+ using the ammonium salt method.

In the sodium vanadate solution after desiliconization by adding $Al_2(SO_4)_3$ and after adding NH_4Cl or $(NH_4)_2SO_4$, the pH remained at ~8. The solubility of the ammonium vanadate increases with the increase in temperature. Consequently, NH_4VO_3 was precipitated at 20–30 °C. Mechanical stirring, or the addition of crystal seeds, accelerates the precipitation efficiency of NH_4VO_3. To complete the precipitation, the solution needs to stand for an extended period. After the precipitation, the slurry was filtered and a 1% ammonium salt solution NH_4Cl was used to wash the solid precipitate, which was then dried at 35–40 °C to obtain ammonium vanadate. Precipitation at high temperatures (80 °C) and crystallization at room temperature increases the precipitation efficiency. The supernatant solution after vanadium precipitation has a concentration of approximately 1–2.5 g/L. The consumption of NH_4^+ ions is excessive, and NH_3 needs to be recycled (0.18 NH_3 per kilogram of V_2O_5). The precipitation method requires the vanadium concentration to be high (30–50 g/L), while there is excessive consumption of ammonium salt.

In this work, precipitation of ammonium vanadate was performed using a vanadium concentration of 30 g/L at a pH of 8. Ammonium salt was added, and the solution was heated to the precipitation temperature. After the precipitation, the reaction solutions were cooled down overnight. The vanadium concentration of the supernatant solution obtained was then analyzed. The precipitation efficiency of ammonium vanadate was calculated based on the vanadium concentration. The

Table 4
Composition of the remnant solution after desiliconization.

Element	Al	Fe	Na	P	S	V	Si
Content g/L	5.71	0.05	16.0	0.23	0.57	11.7	8.27

Table 5
Different vanadium ion species at various pH values.

pH	>13	13–9	9–6.6	6.6–6.0	6.0–3.5	3.5–2	~ 1
Vanadium ion state	VO_4^{3-}	HVO_4^{2-}	$V_3O_9^{3-}$	$V_{10}O_{28}^{6-}$	$HV_{10}O_{28}^{5-}$	$H_2V_{10}O_{28}^{5-}$	VO_2^+

Vanadium concentration is 0.5 g/L (Al-Kharafi and Badawy, 1997).

effect of pH is plotted in Fig. 6. When the pH is in the range of 7.5–8.5, the precipitation efficiency of vanadium is the highest. When the pH is higher, the precipitation efficiency of the vanadium decreases because the ammonium vanadate dissolves back into the solution at high pH. The results show that the optimal pH for precipitation is 8. The ammonium salt was NH_4Cl, and the vanadium precipitation coefficient K calculated using Eq. (8) was 2.

$$K = \frac{\text{The weight of the } NH_4Cl(g)}{\text{The weight of the } V_2O_5(g)} \quad (8)$$

3.3.2. Effect of precipitation coefficient

The effect of the vanadium precipitation coefficient K on the precipitation efficiency is plotted in Fig. 7. When K is between 1.0 and 2.0, the precipitation efficiency increases with K, and when K is larger than 2.0, the precipitation efficiency tends to be steady. The equation for the precipitation of vanadium is as follows:

$$NaVO_3 + NH_4Cl \rightarrow NH_4VO_3 + NaCl \quad (9)$$

As the mole ratio of the $NH_4Cl/NaVO_3$ in the reaction is 1, when K = 2, the mole of the $NH_4Cl/NaVO_3$ is calculated to be 3.43, and K = 2 is determined to be the optimal vanadium precipitation coefficient. Purity of obtained NH_4VO_3 precipitate was determined by XRF, and it was 97.4%. There were some traces of impurities of silicon, iron, aluminum and calcium in the precipitate.

3.3.3. Effect of vanadium concentration and temperature

The effect of the vanadium concentration, given as V_2O_5 concentration, on the vanadium precipitation efficiency is plotted in Fig. 8a. When the vanadium concentration was 15–30 g/L, the vanadium precipitation efficiency increased with the increase in vanadium concentration. When the vanadium concentration was >30 g/L, the precipitation efficiency was steady.

Although the rate of precipitation can be faster at higher temperatures, the precipitation efficiency of ammonium vanadate decreases. As can be seen in Fig. 8b, when the temperature rises from 30 °C to 50 °C, the vanadium precipitation efficiency increases, but when the temperature rises from 50 °C to 70 °C, the precipitation efficiency decreases.

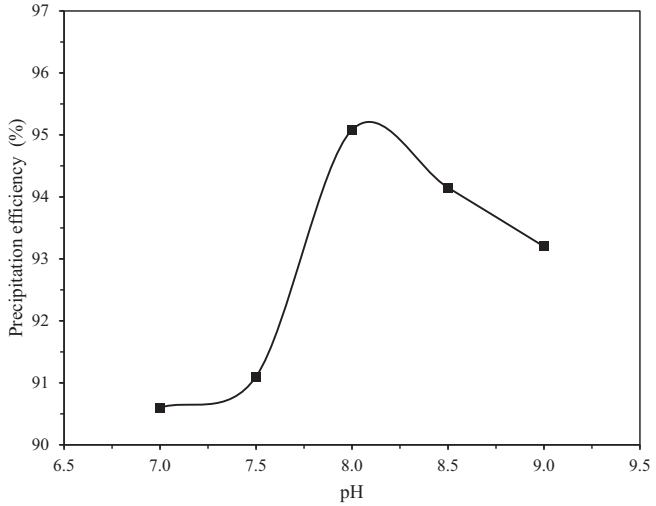

Fig. 6. Effect of pH on precipitation efficiency.

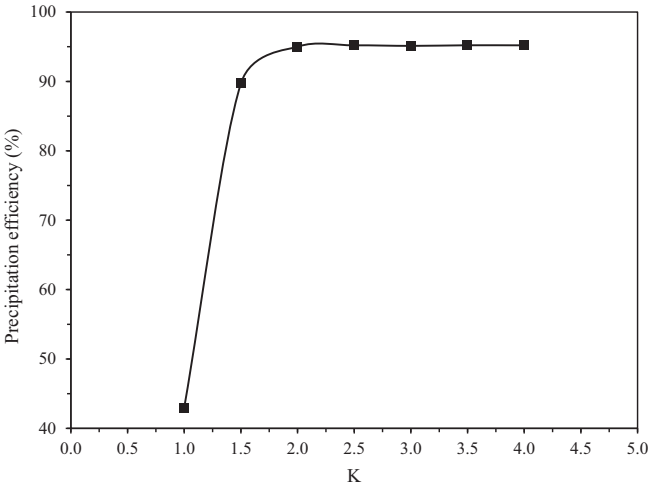

Fig. 7. Effect of the vanadium precipitation coefficient K on the precipitation efficiency.

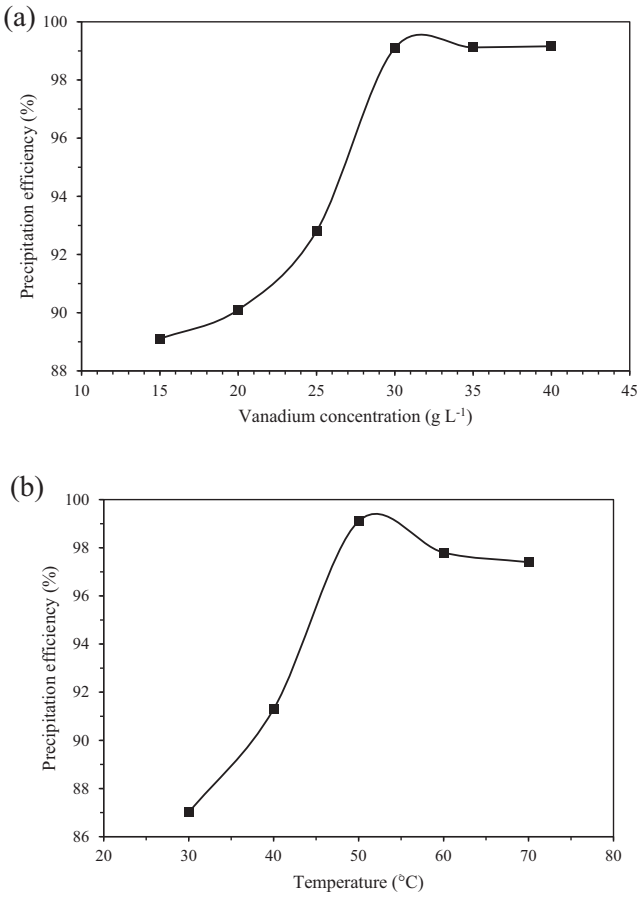

Fig. 8. Effect of a) vanadium concentration and b) temperature on the precipitation efficiency.

This is due to the fact that the solubility of ammonium vanadate increases as a function of temperature above 50 °C.

4. Conclusions

The water leaching of vanadium from soda-roasted vanadium slag was studied, and a 96.9% yield of vanadium was obtained from water leaching at 100 °C. Temperature was the main parameter affecting leaching efficiency, while agitation speed and the liquid-to-solid ratio had only a minor impact. The vanadium solution obtained had a significantly high vanadium content (V_2O_5 52.5 g/L) but also had a residual silicon concentration of 1.67 g/L.

Silicon was significantly removed from the solution via desiliconization. All the parameters studied, such as pH, temperature, and the-$Al_2(SO_4)_3$/Si mass ratio affected the desiliconization process, and it was possible to optimize the conditions for silicon removal without a significant vanadium loss.

Precipitation of ammonium vanadate was performed at an optimal pH of 8.0, a temperature of 50 °C, and a vanadium solution concentration of 30 g/L to maximize the ammonium vanadate yield. Under these conditions, the vanadium precipitation coefficient K was 2. After 300 min of precipitation, a vanadium precipitation efficiency of 99% was achieved. Purity of ammonium vanadate was 97.4%.

CRediT authorship contribution statement

Longjie Liu: Conceptualization, Writing – original draft, Writing – review & editing. **Toni Kauppinen:** Writing – review & editing. **Pekka Tynjälä:** Writing – review & editing. **Tao Hu:** Writing – review & editing. **Ulla Lassi:** Conceptualization, Writing – original draft, Writing – review & editing, Funding acquisition.

Declaration of Competing Interest

The authors declare that they have no known competing financial interests or personal relationships that could have appeared to influence the work reported in this paper.

Acknowledgments

This research was funded by the ADCHEM project, Tekes (grant number: 1792/31/2016).

References

Al-Kharafi, F.M., Badawy, W.A., 1997. Electrochemical behavior of vanadium in aqueous solutions of different pH. Electrochim. Acta 42 (4), 579–586. https://doi.org/10.1016/S0013-4686(96)00202-2.

Chen, G., et al., 2013. An investigation on the kinetics of chromium dissolution from Philippine chromite ore at high oxygen pressure in KOH sub-molten salt solution. Hydrometallurgy 139, 46–53. https://doi.org/10.1016/j.hydromet.2013.07.004.

Ji, Y., et al., 2017. Cleaner and effective process for extracting vanadium from vanadium slag by using an innovative three-phase roasting reaction. J. Clean. Prod. 149, 1068–1078. https://doi.org/10.1016/j.jclepro.2017.02.177.

Li, H.-Y., et al., 2016. Selective leaching of vanadium in calcification-roasted vanadium slag by ammonium carbonate. Hydrometallurgy 160, 18–25. https://doi.org/10.1016/j.hydromet.2015.11.014.

Liu, B., et al., 2013. A novel method to extract vanadium and chromium from vanadium slag using molten NaOH-$NaNO_3$ binary system. AICHE J. 59 (2), 541–552. https://doi.org/10.1002/aic.13819.

Liu, L., et al., 2017. Intensified decomposition of vanadium slag via aeration in concentrated NaOH solution. Int. J. Miner. Process. 160, 1–7. https://doi.org/10.1016/j.minpro.2017.01.003.

Lübke, M., Ding, N., Powell, M.J., Brett, D.J.L., Shearing, P.R., Liu, Z., Darr, J.A., 2016. VO2 nano-sheet negative electrodes for lithium-ion batteries. Electrochem. Commun. 64, 56–60. https://doi.org/10.1016/j.elecom.2016.01.013.

Macdougall, G.J., et al., 2012. Magnetic order and ice rules in the multiferroic spinel FeV_2O_4. J. Phys. Rev. B 86 (6), 6709–6717. https://doi.org/10.1103/PhysRevB.86.060414.

Wei, Z., Liu, D., Hsu, C., Liu, F., 2014. All-vanadium redox photoelectrochemical cell: an approach to store solar energy. Electrochem. Commun. 45, 79–82. https://doi.org/10.1016/j.elecom.2014.05.018.

Yan, X., et al., 2017. A novel imidazolium-based amphoteric membrane for high-performance vanadium redox flow battery. J. Membr. Sci. 544, 98–107. https://doi.org/10.1016/j.memsci.2017.09.025.

Yang, Z., et al., 2014. Leaching kinetics of calcification roasted vanadium slag with high CaO content by sulfuric acid. Int. J. Miner. Process. 133, 105–111. https://doi.org/10.1016/j.minpro.2014.10.011.